

# Quadrature Tomographic Microscope Project Narrative

## 1 Introduction

This CenSSIS project combines research in (1) cell biology, (2) interferometry, (3) light scattering, and (4) limited-view tomography. A new type of microscope, a Quadrature Tomographic Microscope (QTM), has been developed to obtain two-dimensional images of magnitude and phase of the electric field at a wavelength of 633 nm for imaging unstained biological specimens. Our model biological system for QTM imaging is mouse oocytes and embryos. The long-range goal is to use the QTM for imaging of human oocytes and embryos from IVF clinics in order to noninvasively assess viability. In addition, the QTM will likely have other biological applications, such as differentiating cancerous from normal cells. Multiple images from the QTM may be combined tomographically to produce three-dimensional maps of the complex index of refraction. Parameters of the oocyte or embryo (or other biological specimen) are then derived from the images. In an alternative approach, the parameters are obtained directly from the 2-D images, without the intervening 3-D image. For year 2, we plan to construct the third-generation microscope (QTM-III). We will continue to compare QTM images with other microscopic images to determine the significance of our chosen contrast parameters. We will also continue to develop theoretical models for predicting our ability to detect these parameters, and will begin to develop inversion algorithms to obtain them.

## 2 Biological Rationale

The initial success of IVF in man [1] has led to an IVF industry that has produced more than 300,000 IVF babies worldwide. However, the success rate of producing live babies from IVF is only about 20%, largely due to the inability to properly assess embryo quality using present microscopic imaging systems. Women undergoing IVF are treated with hormones so that they produce up to 20 oocytes per hormone cycle. After fertilization and several days of culture, the “best” embryos must be chosen for transfer back to the mother. At the present time, using conventional microscopy, it is not possible to determine which “normal” appearing embryos are viable. This was highlighted in a recent article on human embryo research[2] that states, “In producing embryos for transfer to the patient, infertility doctors often find themselves faced with too many fertilized eggs. Generally they choose the best-looking embryos for implantation. But investigators are finding that the best-looking embryos are not always normal.”

Another problem with current IVF practices is that multiple embryos are usually re-introduced into the mother. This has led to a large number of twin and triplet births, leading to great physical and emotional stress on the mothers who are often in their late 30s or early 40s. Moreover, a recent paper has reported that the incidence of cerebral palsy among IVF triplets is 24%[3], making it highly desirable to be able to choose the best single embryo for implantation back into the mother. The prospect of single blastocyst transfer after IVF is being explored[4], but although this will alleviate the multiple birth problem, the success rate of IVF after single blastocyst transfer is still about 20%. Clearly, new imaging techniques that could provide a scientific, quantitative means to assess oocyte and embryo quality would be a major breakthrough.

## 3 Assessment of Oocyte and Embryo Viability with the QTM

As in all subsurface imaging, the basic question is about contrast: “What contrast features that distinguish viable mammalian embryos from others can be measured noninvasively?” From the biologist’s perspective, the first question is when to assess the embryo. Different parameters are observable in the oocyte (e.g. expansion and radiance of cumulus cells, meiotic status, polar-body morphology, refractile bodies, vacuoles, darkened or unhealthy cytoplasm, fractured zona pellucida, large perivitelline space), in the zygote (e.g. number, polarization, and symmetry of nucleolar precursor bodies), and more developed embryos (e.g. symmetry/size of blastomeres, fragments in perivitelline space, quality of cytoplasm, embryo-development ratio).

---

<sup>1</sup>2531nc.tex — 12 March 2001 at 17:14

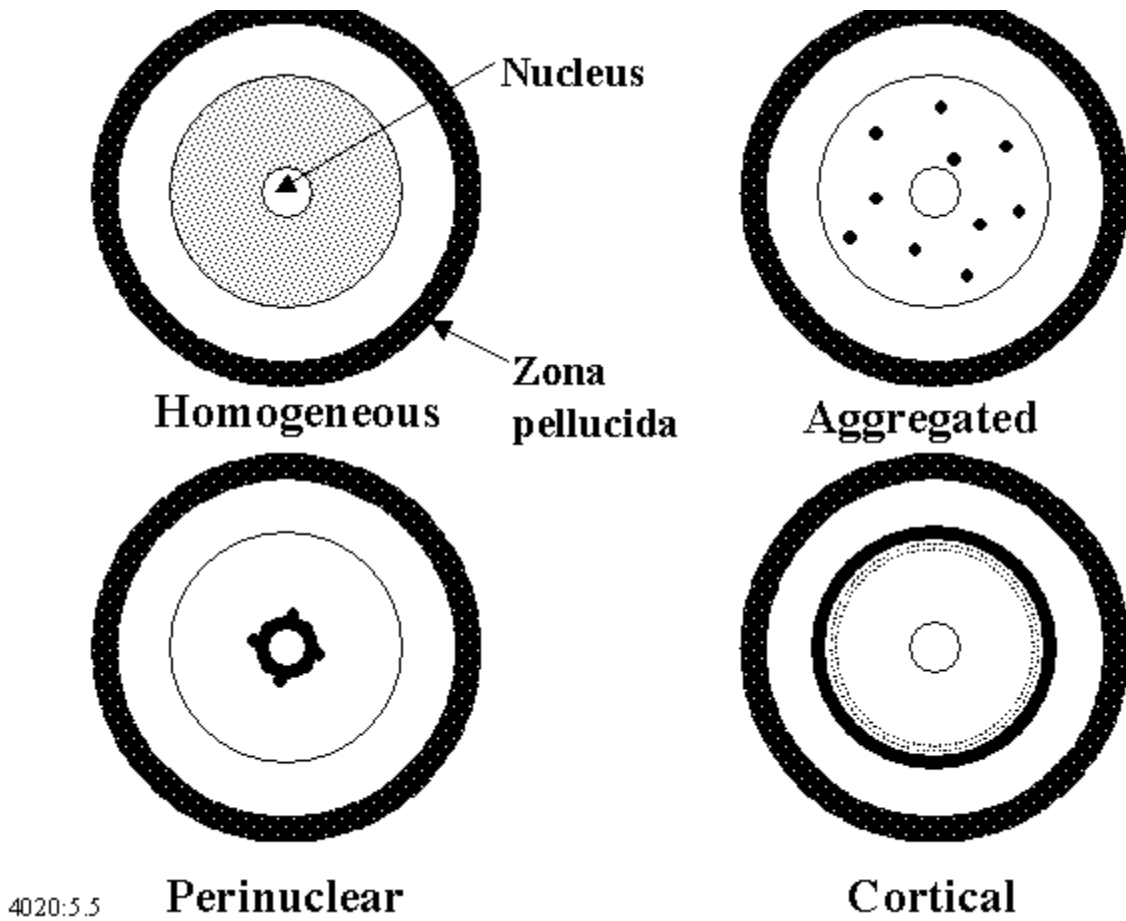


Figure 1: Distributions of Mitochondria.

These parameters have been chosen primarily because they are visible with existing non-invasive imaging, rather than for their fundamental relationships to viability.

## 4 Mitochondrial Distribution

In contrast, it is known that mitochondria play a significant role in the development of mammalian oocytes and embryos[5, 6, 7, 8]. They produce energy and are thus located in areas of high energy demand within the cell. Defective or low numbers of mitochondria are correlated with reduced developmental capacity. Mouse oocytes contain about 92,500 mitochondria which are somewhat ellipsoidal with a major axis of 1.5 micrometers and a minor axis of 0.5. Assuming an index of refraction of 1.42 for mitochondria and 1.37 for cytoplasm[9], scattering cross-sections are of the order of 0.2 square micrometers with strong forward scattering ( $g > 0.95$ ). If they are packed homogeneously in a 70-micrometer diameter cell body (although, as discussed below, this is not necessarily true), the scattering coefficient would be around 500 inverse centimeters (comparable to that of tissue). Although there is significant scatter ( $\mu_s \ell \approx 4$ ), most of it is forward ( $\mu_s(1-g)\ell \approx 0.2$ ) and the embryo, even in this case, looks quite transparent.

The mitochondria are, in fact, not always homogeneously distributed, and their distribution changes with growth. In the oocyte, the mitochondria change from a homogeneous distribution to a perinuclear one. Aggregation in the cytoplasm has also been observed, as has a compact, cortical distribution. It is not presently certain which types of mitochondrial distribution are indicative of embryo health. The four types of mitochondrial distribution that have been described are shown in Figure 1. We will assess mitochondrial distribution in mouse oocytes and embryos by labeling the mitochondria with fluorescent dyes and imaging

them by using confocal microscopy. Dr. Donald O'Malley at NU will assist us with the confocal imaging procedures. We will also use the 2-photon scanning laser microscope available through Dr. David Golan at BWH to assist in the determination of the "ground truth" of mitochondrial distribution in oocytes and embryos.

Then these mitochondrial distribution patterns will be compared to the images obtained with the QTM. Since the mitochondria in the oocytes and embryos do not need to be stained for analysis with the QTM, we should be able to compare mitochondrial distribution patterns with viability. Viability of oocytes will be assessed by the ability of oocytes to be fertilized and develop to the blastocyst stage. Viability of embryos is more complicated to assess than viability of oocytes. We will assess viability of embryos by the ability to generate live offspring after embryo transfer to foster mothers. These experiments will be undertaken in later years of this project.

An interesting point is that aggregation of several mitochondria will produce a scattering cross-section less than the sum of that of the individual ones, and with a very different angular distribution. Mitochondria can be resolved with a high-magnification microscope, but because of their number, resolving all of them would be a formidable task, and success would lead to the question, "What do we do with all this information?" We plan an alternative approach. The far-field angular distribution of light from a single scatterer contains information about its composition, size, and shape. The field from multiple scatterers is the sum of the individual contributions. Spatial filtering can be employed to limit the number of scatterers observed in a single measurement. Because the QTM measures the complex field, we can, to some extent, collect a single image and perform transformations to do spatial filtering and examine the far-field patterns. Because the patterns depend on size, shape, and composition, ambiguity normally results. The use of multiple wavelengths may resolve this, and is easily implemented in the QTM. Thus, it seems likely that we can set a goal of determining mitochondrial distribution without the intervening step of full 3-D imaging.

## 5 Model Building

In order to understand how to collect and process the appropriate images, we need a model of how light propagates in a cell. Because of the amount of scattering, it is not likely that a single-scatter model will be sufficient. We plan to use a model developed at the University of Texas by Andrew Dunn, presently at the MGH NMR Center[9], to compute the images which will be seen by the QTM. The model was designed for cells having a diameter of about 10 wavelengths, but advances in computers since that time have made it possible to use it up to about 50 wavelengths. We plan to use the computing power of CenSSIS to reach the goal of more than 100 wavelengths. The present program produces the angular distribution of the field over a hemisphere. We plan to modify the output routine to calculate images in a smaller area, representing the objective lens of the QTM, and to propagate these to the image plane using a Fresnel-Kirchoff integral. Consideration will be given to multiple views, and views where the directions to the light source and the imager are not parallel. This gives rise to an interesting limited-view tomography problem, in which (1) for a single illumination direction, multiple non-contiguous patches of image may be available, (2) a limited number of illumination directions will be available, (3) illumination may not be with plane waves, (4) multiple wavelengths may be used for each view, and (5) the goal will be to determine a limited set of parameters for mitochondrial distribution, e.g. homogeneous, aggregated, perinuclear, or cortical as was shown in Figure 1.

## 6 Cell Count

The next parameter we plan to study, which is known to affect embryo viability, is cell count (reviewed in Warner and Brenner, 2001[10]) When the oocyte is fertilized it becomes a zygote, which then divides to become a two-cell embryo. Each of these cells then divides, and the process continues to the blastocyst stage (approximately 32 cells in the mouse), and only after this stage does the embryo begin to grow in total size. Because the timing of cell division is random after the two-cell stage, any number of cells is possible. In the blastocyst, cells are differentiated as being outer cells, the trophectoderm (TE) or inner cells, the inner cell mass (ICM), as shown in Figure 2. The ICM gives rise to the fetus whereas the TE gives rise to the placenta. The number of cells in the ICM has been related to embryo viability[11, 12, 13, 14, 15] However, the complexity of the embryo at this stage makes cell counting difficult. In contrast to the cells of the early

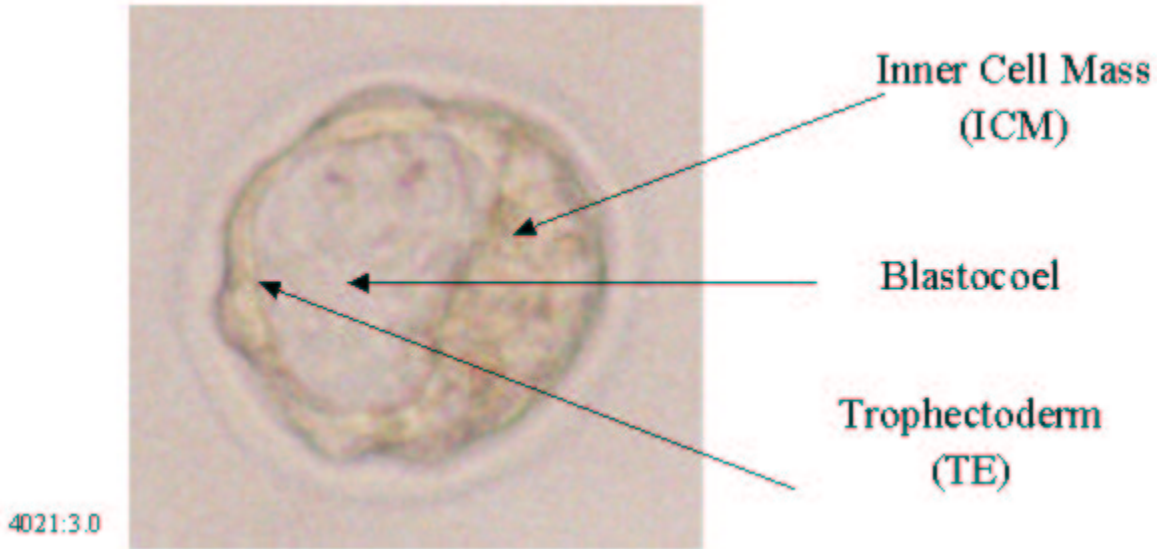


Figure 2: Blastocyst showing the major components.

embryo, those of the blastocyst are highly scattering, and imaging through the TE to see the ICM is difficult, if not impossible, without staining the embryo and thereby compromising its viability.

Again, this presents an interesting imaging problem. The resolution requirement is quite modest, as we are looking for approximately 32 cells in a volume of 100 cubic wavelengths. The challenge is to process the data in such a way as to “hide” all the detailed information about cell nuclei, mitochondria, and other “clutter” so that the cells may be counted. Some information must be retained, of course, to distinguish the ICM from the trophectoderm. Here again, multiple wavelengths may be useful, particularly to penetrate the trophectoderm, using techniques borrowed from diffusive optical tomography. It is evident that this clutter rejection task is not unlike the task of imaging landmines through a rough ground surface using ground-penetrating radar. The model we use for the mitochondrial density imaging will be used with different inputs to produce a model for the blastocyst. We will construct a model in which cells are spheres of differing sizes within the embryo, and each sphere contains a nucleus and a different distribution of mitochondria.

## 7 The QTM

The QTM is an interferometric instrument that measures both amplitude and phase. In conventional interferometry, light which interacts with the specimen mixes with a reference wavefront to produce an irradiance

$$I_+ = |U|^2 = |U_{spec} + U_{ref}|^2 = |U_{spec}|^2 + |U_{ref}|^2 + 2\Re[U_{spec}U_{ref}^*], \quad (1)$$

where  $U$  is the total field amplitude,  $U_{spec}$  is the amplitude contributed by the specimen path and  $U_{ref}$  is the amplitude contributed by the reference path.

The first advantage of coherent detection is the ability to approach the fundamental limit of optical imaging. Because  $U_{spec}$ , which contains information about the specimen is multiplied by  $U_{ref}$ , the measured signal can be increased without increasing exposure of the specimen, by increasing the reference power. In this way, the QTM can overcome detector noise and approach the fundamental limit more easily than can incoherent detection, which can only observe  $|U_{spec}|^2$ .

The second advantage of coherent detection is that it is sensitive to phase, and can thus distinguish different parts of a specimen using a wavelength that is not absorbed significantly by any part of the specimen. Thus, most of the incident light is detected rather than absorbed in the specimen, reducing the potential for toxicity.

Conventional interferometry produces ambiguous results, however, because it can not distinguish between changes in amplitude and changes in phase (See Equation 1). Quadrature interferometric imaging[16]

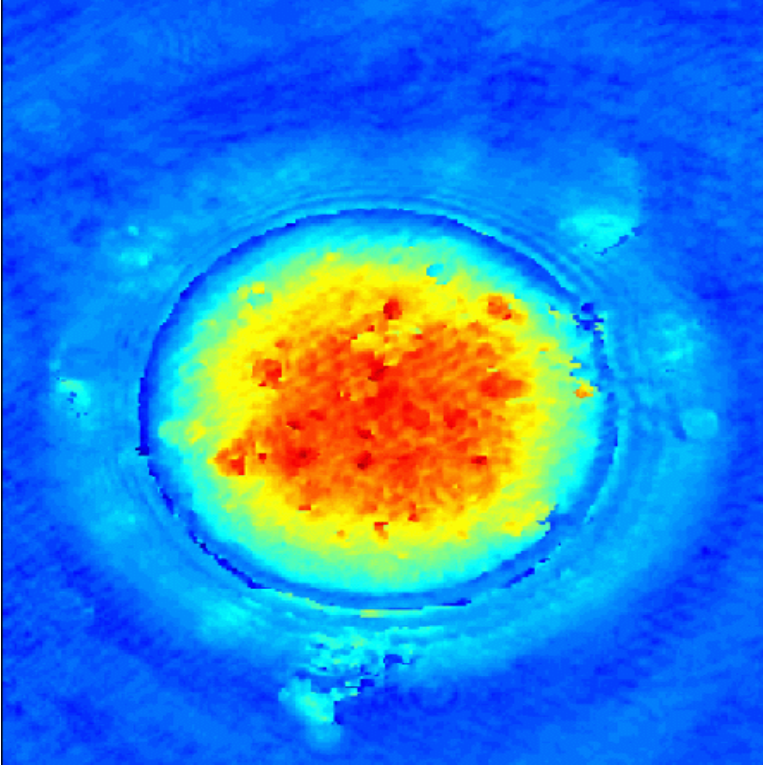


Figure 3: Phase image (unwrapped) of mouse oocyte.

overcomes this limitation by obtaining at least two images with different phases for the reference. In fact, in the current QTM, four images are used. Two images are obtained by mixing the linearly polarized signal with a circularly polarized reference generated by the quarter-wave plate in the figure, and selecting two polarizations at  $\pm 45$  degrees to the signal polarization. Both outputs of the interferometer are used in a balance-mixer configuration, common in coherent radar, producing two more images. At one output, the signal is  $U_{spec} + U_{ref}$ , while on the other it is  $U_{spec} - U_{ref}$ . The polarizers separate the in-phase and quadrature channels and the detectors produce signals proportional the square of the amplitudes;

$$I_+ = |U_{spec}|^2 + |U_{ref}|^2 + \Re[U_{spec}U_{ref}^*], \quad (2)$$

$$I_- = |U_{spec}|^2 + |U_{ref}|^2 - \Re[U_{spec}U_{ref}^*], \quad (3)$$

$$Q_+ = |U_{spec}|^2 + |U_{ref}|^2 + \Re[U_{spec}(U_{ref}e^{i\pi/2})^*], \quad (4)$$

$$Q_- = |U_{spec}|^2 + |U_{ref}|^2 - \Re[U_{spec}(U_{ref}e^{i\pi/2})^*]. \quad (5)$$

Thus, we can obtain an estimate of the total field from the specimen as viewed at a particular pixel in the detector;

$$\hat{U}_{spec} = \frac{(I_+ + I_-) + i(Q_+ + Q_-)}{U_{ref}^*}. \quad (6)$$

The reference field,  $U_{ref}$  can be known only to within a constant of unit amplitude, as its absolute phase is unknown, so  $U$  in Equation 3 is the complex field amplitude multiplied by this unknown constant.

The present table-top implementation (QTM-II) has produced the images we have shown to date, (an example is shown in Figure 3 but it is not sufficient to produce images which can be of great use to the

biologist. Thus we plan to develop QTM-III on a microscope body, with collimated laser illumination. The laser will be directed to the illumination path through a single-mode optical fiber splitter. The other output of the splitter will be directed to an assembly of beamsplitters and four cameras like that on the QTM-II, except that these will be placed in the camera port of the microscope. Because the fiber splitter has a second input, it will be easy to implement a two-wavelength QTM. Because the fiber will act as a spatial filter, many of the optical artifacts caused by the beam profile in the present system will be eliminated. Furthermore, the use of a commercial microscope body and higher quality objectives will reduce the aberrations which limit the present system. Finally, the use of a commercial microscope body will make it easy to change objectives to obtain different magnifications, and will permit the use of a heated, perfused stage so that the specimens can be kept alive for long imaging sessions.

## 8 Data Processing Algorithms

We will begin development of inversion algorithms, along the lines we have discussed in a proposal that we submitted to the NIH, which is under revision for resubmission. It is important to optimize the reconstruction process to maximize information extraction and minimize cell exposure. In our attempt to minimize cell exposure we are led to imaging kernels for the QTM that provide nonlocal information about the spatial distribution of the specimen (unlike *e.g.* confocal microscope images). In particular, these kernels have tomographic-like characteristics, and produce challenging inverse problems [17, 18].

Inversion methods popular in medical tomography (*e.g.* filtered back-projection), are based on the exact Radon inversion formula, which assumes the presence of a set of high-quality data with complete angular coverage [17]. These methods are known to work poorly with limited data, however, due to the fact that they ignore the actual acquisition geometry and physics responsible for the data. In contrast, by using the models we will develop as the basis for inversion, we are able to take such information into account and can produce useful inversions even in the face of limited and low quality data. We have successfully performed such data inversion in problems of atmospheric tomography and synthetic aperture radar imaging [19, 20, 21]. The price for such a model-based approach is computational. Indeed, since some of the kernels developed in our preliminary analysis of the problem have a large effective support, the computational load during inversion can be high if the exact forward model is used as is.

To meet this computational challenge, we will take a two prong approach. First, we will develop rational approximations of the imaging operator based on our understanding of the physics of the problem. For example, the coherent detection process will allow us to combine data from adjacent pixels to generate “custom kernels” which may have shapes which simplify the inversion problem. One such combination produces a kernel similar to that of x-ray tomography, which can be inverted simply, but suffers from poor resolution. Another combination can change the focus[22]. These kernels can produce a “coarse image,” which can be used to reduce the computational load for processing images using the nonlocal kernels. Second, we can make use of the fact that our actual information needs are much less than complete reconstruction. For example, a typical image is less than a million pixels. If we reconstruct 0.25-micrometer voxels in a 100-micrometer cube, this requires 64 million voxels, making the problem very underdetermined. On the other hand, if we wish to determine the mitochondrial density in voxels of 10 micrometers, we have only 1000 unknowns, and the problem is in some sense overdetermined. The challenge is to ensure that unwanted details do not contaminate the desired 1000 measurements.

This project contains two challenging tasks in computing requirements: the forward model and the data collection and processing. We will work with Profs. Kaeli and Meleis on the model. With Prof. Manolokos we will explore the potential use of Javaports for the latter task.

## 9 Conclusion

In summary, we have found two parameters, mitochondrial distribution and cell count in the ICM, which are likely coupled to oocyte and embryo viability, are observable with the QTM, are difficult to observe non-invasively otherwise, and pose challenging but solvable problems in modelling, image reconstruction, and data management.

## References

- [1] P. C. Steptoe, R. G. Edwards, , and J. M. Purdy, “Clinical aspects of pregnancies established with cleaving embryos grown *in vitro*,” *Br. J. Obs. Gyn.* **87**, pp. 757–768, 1980.
- [2] S. Latta, “Reproductive research progresses despite restrictions,” *The Scientist* , March 1998.
- [3] N. M. Fisk and G. Trew, “Two’s company, three’s a crowd for embryo transfer,” *Lancet* **354**, pp. 1572–1573, 1999.
- [4] D. K. Gardner, M. Lane, T. Pool, and W. B. Schoolcraft in *ART and the Human Blastocyst Serono Symposium*, Scientific Committee, 2000.
- [5] A. Fukada, K. F. Breuel, and S. S. Thatcher, “Localization and density of mitochondria in the mouse embryos developed *in vivo* and *in vitro*,” *Human Reproduction* **128**, 1993.
- [6] T. Tokura, Y. Noda, Y. Goto, , and T. Mori, “Sequential observation of mitochondrial distribution in mouse oocytes and embryos,” *Journal of Assisted Reproduction and Genetics* **10**(6), pp. 417–426, 1993.
- [7] J. M. Squirrell, D. L. Wokosin, J. G. White, and B. D. Bavister, “Long-term two-photon fluorescence imaging of mammalian embryos without compromising viability,” *Nature Biotechnology* **17**, pp. 763–767, 1999.
- [8] A. H. Sathananthan and A. O. Trounson, “Mitochondrial morphology during preimplantational human embryogenesis,” *Human Reproduction* **15**(2), pp. 148–159, 2000.
- [9] A. Dunn and R. Richards-Kortum, “Three-dimensional computation of light scattering from cells,” *IEEE Journal of Special Topics in Quantum Electronics* **15**, p. 898, Dec 1996.
- [10] C. M. Warner and C. A. Brenner, “Genetic regulation of preimplantation embryo survival,” *Current Topics in Developmental Biology* , 2000.
- [11] P. P. Tam, “Postimplantation development of mitomycin c-treated mouse blastocyst,” *Teratology* **37**, pp. 205–212, 1988.
- [12] D. R. Brison and R. M. Schultz, “Rt-pcr-based method to localize the spatial expression of genes in the mouse blastocyst,” *Mol. Reprod. Dev.* **44**, pp. 177–178, 1996 1996.
- [13] M. Lane and D. K. Gardner, “Effect of incubation volume and embryo density on the development and viability of mouse embryos *in vitro*,” *Human Reprod.* **7**, pp. 558–562, 2000.
- [14] A. V. Soom, M. T. Ysebaert, , and A. de Kruif, “Relationship between timing of development, morula morphology, and cell allocation to the inner cell mass and trophectoderm in *in vitro*-produced bovine embryos,” *Mol. Reprod. Dev.* **47**, pp. 47–56, 1997.
- [15] A. W. S. Chan, T. Domjinko, C. M. Luetjens, E. Neuberand, C. Martinovich, L. Hewitson, C. R. Simerly, and G. P. Schatten, “Clonal propagation of primage offspring by embryo splitting,” *Science* **287**, pp. 317–319, 2000.
- [16] D. O. Hogenboom, C. M. Warner, Y. Glina, and C. A. DiMarzio, “Phase imaging of embryos using a quadrature interferometry microscope,” in *Three-Dimensional and Multidimensional Microscopy: Image Acquisition and Processing VI*, No. 3605A in SPIE, pp. 101–106, May 1999.
- [17] A. C. Kak and M. Slaley, *Principles of Computerized Tomographic Imaging*, IEEE Press, Piscataway, N.J., 1987.
- [18] M. Bertero, “Advances in electronics and electron physics,” vol. 75, ch. Linear Inverse and Ill-Posed Problems, pp. 1–120, Academic Press, 1989.

- [19] F. Kamalabadi, J. L. Semeter, W. C. Karl, D. M. Cotton, T. A. Cook, and S. Chakrabarti, "Space-based ionospheric remote sensing using tomographic inversion of radiative recombinative euv sources," *Annual NSF Conference on Coupling, Energetics, and Dynamics of Atmospheric Regions*, June 1997.
- [20] M. Cetin and W. C. Karl, "A statistical tomographic approach to synthetic aperture radar image reconstruction," *Proceedings of the International Conference on Image Processing*, October 1997.
- [21] F. Kamalabadi, W. C. Karl, J. L. Semeter, D. M. Cotton, T. A. Cook, and S. Chakrabarti, "A statistical framework for space-based euv ionospheric tomography," *Radio Science* **34**(2), pp. 437–447, 1999.
- [22] J. J. Stott, R. E. Bennett, C. M. Warner, , and C. A. DiMarzio, "Three-dimensional imaging with a quadrature tomographic microscope," in *Three-Dimensional and Multidimensional Microscopy: Image Acquisition and Processing VIII*, No. 4261 in SPIE, p. TBD, January 2001.